Hole stabilization and recombination in solid Ar investigated by low-energy electron stimulated desorption of neutral particles

E. Vichnevetski,* A. D. Bass, P. Cloutier, and L. Sanche†
Groupe des Instituts de Recherche en Santé du Canada en Sciences des Radiations, Dép. Médecine Nucléaire et Radiobiologie, Faculté de Médecine, Université de Sherbrooke, Sherbrooke, Qc, Canada, J1H 5N4
(Received 24 September 2003; published 20 February 2004)

Positive charge creation and annihilation induced by low-energy electron impact in thin Ar films (20–180 monolayers) is investigated within the 5–30-eV range by measuring the desorption of metastable particles, the emission of UV photons, and the threshold energies for these processes. The mechanisms of charge formation and electron-hole recombination are determined from measurements of the charge/discharge dependence on the duration and energy of electron irradiation. The accumulation of positive charge results from the trapping of holes in the lattice, principally at the film/vacuum interface. The localization of these holes is stable at 20 K and their migration within the Ar film after irradiation is practically absent. After electron bombardment with electrons of energy $E_{\mathrm{irr}} \geqslant 13$ eV, the positively charged films can be discharged if irradiated by electrons of lower energy. Film discharging is dominated by a single process, mainly the recombination of Ar_2^+ centers with near thermal energy electrons.

DOI: 10.1103/PhysRevB.69.085408 PACS number(s): 73.50.Gr, 34.80.Dp, 34.80.Kw

INTRODUCTION

The rare-gas solids (RGS's) possess the widest band gap of all materials and provide attractive model systems for studying electronic relaxation processes in irradiated insulators. Studies of these materials have thus enlarged our understanding of the interconnections between electronic and atomic processes involved in such fundamental problems as hole self-trapping,[1] the prominent role of holes in electronically induced phenomena,[2,3] charge transport, and energy storage.[4]

Charge accumulation within and near the surfaces of dielectric solids following exposure to ionizing irradiation is a well-known effect that has attracted interest across scientific and technological fields.[5,6] Unsurprisingly, the phenomenon has also been observed, sometimes coincidentally, in the rare-gas solids. For example, electrostatic effects due to the accumulation of positive charge (''positive charging'') by RGS's were observed[7] when Ar, Kr, and Xe films were irradiated by 10–100-keV protons. More generally, the positive charging of thin Ar films condensed onto a metallic substrate may also be produced by any ionizing radiation of energy greater than the Ar band gap ($E_g = 14.16$ eV). The absorption of such radiation results in the appearance of an equal number of free electrons and holes, but since the mobilities of electrons in RGS's exceed those of holes by factors $10^4 - 10^5$,[1] and the mean free paths are similarly greater due to paucity of energy-loss processes below the onset of the exciton formation, a significant fraction of the free electrons may scatter into the metallic substrate or into vacuum.[7,8] Holes rapidly self-trap due to their strong interaction with acoustic phonons[9,10] and stabilize as Ar_2^+ centers, that may subsequently recombine with available free electrons. A net imbalance in the number of stabilized holes and electrons remaining in the film permits the accumulation of a positive charge.

On the other hand, electron bombardment of RGS's below the ionization threshold may result in the accumulation of negative charge via electron trapping at defects or impurities, e.g., in Ref. 11 it is shown that electrons become attached to surface adsorbed oxygen, as O_2^- and O^-. Since impurities are present in even the highest research grade rare gases, it is possible that electron attachment to impurities represents a fraction of the electron traps observed in the thermally activated emission of electrons from electron-irradiated rare-gas films.[10] Nevertheless, most electron traps are shallow and associated with structural defects, as demonstrated by the very low temperatures (<15 K) required to empty these traps in measurements of thermally stimulated luminescence and electron emission.[8,10,12] There are, however, still significant gaps in our knowledge on how the behavior of both electrons and holes within the RGS's affects both luminescence and desorption.[8,13,14]

Many experiments have been performed on ionization and charge recombination in insulators induced by bombardment with high-energy particles, including electrons.[7,9,15,16] These studies, however, do not provide a detailed description of the intermediate processes involved. High-energy particles produce ions and large quantities of secondary electrons, which further interact with the medium. Most of these secondary electrons have energies below 20 eV. It is therefore of interest to study the interaction of such electrons with RGS's to gain further insight into the details of the mechanisms of charging and charge recombination in RGS's. Our study uses electron-stimulated desorption (ESD) to measure positive charge accumulation in rare-gas solids. In this paper, we present a study on the ionization of Ar by electrons within the range 9–30 eV. Not only can these electrons positively charge the solid, but they can, despite their high kinetic energies, also contribute to charge annihilation via electronic excitation. We present the results of ESD experiments on 20–180-monolayers (ML's)-thick Ar films which have been condensed directly onto Pt(111) or upon n-hexane crystalline films of 3- and 10-ML thickness. These Ar films were preirradiated by electrons with $E_{\mathrm{irr}} \geqslant 13$ eV and afterwards bom-

barded by electrons with $E \leqslant 12.0$ eV. We have measured the yield of neutral particles (NP's, i.e., photons and metastables species) emitted and desorbed by during this second electron bombardment.

EXPERIMENT

Experiments were performed in an ultrahigh vacuum (UHV) system capable of reaching a base pressure $\sim 4 \times 10^{-11}$ Torr.[17] The apparatus consists of an electrostatic cylindrical monochromator, a cryogenically cooled Pt(111) substrate, and hemispherical low-energy electron diffraction (LEED) grids followed by a position sensitive detector. The Pt single crystal can be cooled to 20 K and cleaned by electrical heating at temperatures >1000 K and/or Ar bombardment. In the present experiments, an alternative crystalline *n*-hexane (nH_c) substrate was prepared by depositing *n*-hexane onto the platinum at 70 K. At this temperature a crystalline surface is formed that limits diffusion of Ar overlayers into the *n*-hexane layer and separates the adsorbate from the metal.[18] Experiments were performed with well-collimated low-energy (0.2–30 eV) electrons which strike the target at 18° with respect to the surface normal. The electron beam current is 5 nA and the energy resolution 60 meV. The energy of the electron beam is calibrated relative to vacuum level to ± 0.2 eV by comparing the structures in the current transmitted through the argon film, recorded as a function of the incident energy, with previously published data.[19,20] Suitable potentials were applied to the mesh grids to ensure that only neutral particles (i.e., photons and/or metastable atoms and molecules) can be detected. The photon/Ar* ratio in a desorption yield function depends on Ar film thickness and electron impact energy.[21] The threshold energy for detection of NP's is estimated to be ~ 6 eV.[22] Pulsing the electron beam permits time-of-flight (TOF) measurements and/or the separation of photon and metastable signals. However, due to low count rates, most of the data presented here represent combined photon/metastable yields whose variation with incident electron energy is referred to as NP excitation functions.

Target films are grown on the Pt(111) or nH_c substrate by condensing gaseous argon at a temperature of 20 K with a deposition rate of ~ 5 ML's/min. Previous work has shown that this procedure permits the layer-by-layer[23] growth of an fcc argon film having the (111) plane along the film-vacuum interface.[24] From measured LEED patterns, the argon film has been found to consist of domains with a lattice parameter of 5.3 ± 0.2 Å.[17] For these experiments the argon gas was supplied with a stated purity of 99.9995%. The stated purity of n-hexane was superior to 99%. The film thickness (L) was estimated to $\approx 30\%$ accuracy from the calibrated amount of gas needed to deposit a monolayer, assuming no change of the sticking coefficient for the adlayers, as previously described.[17,25] This assumption is supported by direct observation of layer-by-layer growth from interference structures seen in low-energy electron transmission measurements.[23] The reproducibility is estimated to be $\pm 10\%$. In this paper, films of Ar deposited onto Pt or onto *n*-hexane are labeled Ar/Pt or Ar/nH, respectively. A prefix number indicates the amount of deposited component in units of monolayers (e.g., 20Ar/3nH_c for the equivalent of 20 monolayers of Ar condensed on a 3-ML crystalline *n*-hexane film). The ESD experiments themselves are always performed at 20 K. Since in many of these experiments positive charge is produced in the Ar films, the energy of electrons arriving at the film can change during measurement. Note then that unless otherwise stated, the quoted incident electron energies and energy axes of figures refer to the nominal electron energy for an uncharged film (i.e., prior to of electron bombardment).

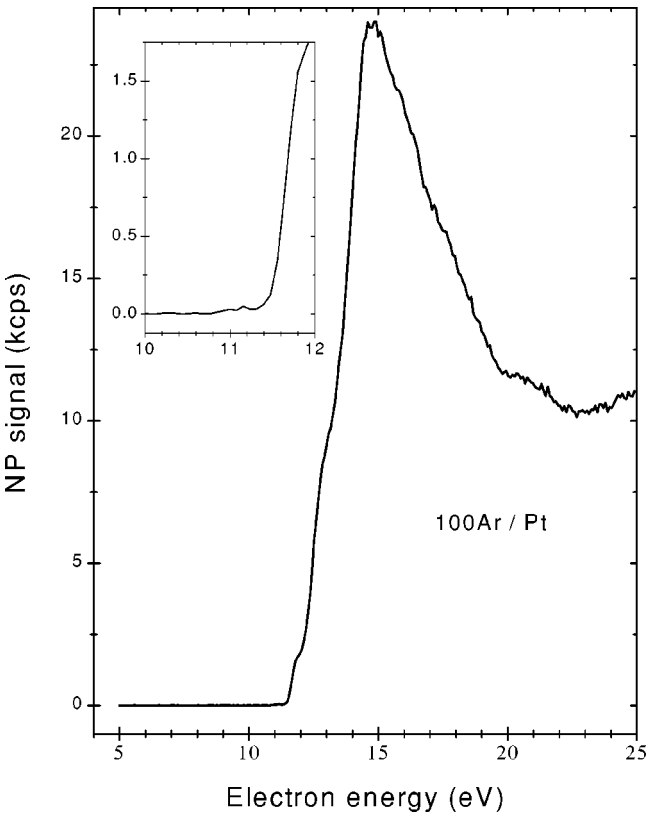

FIG. 1. Neutral particle (NP) yield for a 100-Ar/Pt film as a function of incident electron energy. Inset: The threshold of the same excitation function.

RESULTS

The NP yield function for a 100-ML Ar film condensed onto the Pt(111) substrate is shown in Fig. 1. The desorbed signal and photon luminescence are dominated by contributions from the decay of the atomic and molecular self-trapped excitons (*a*-STE and *m*-STE, respectively).[1,17,26,27] The yield function displays a sharp threshold at ~ 11.5 eV (inset in Fig. 1) and a broad structure with maximum at ~ 15 eV, i.e., at the energy for optimum production of electronic excited states in gas[28] and condensed[17,20] phases. Additionally, two shoulders are observed at ~ 12 and ~ 13 eV; they are associated with the onset of $n=1$ and 2 bulk and surface exciton formation.[26] For thinner Ar films (<10 ML's) deposited onto substrates where the bottom of the conduction band "V_0^S" lies more than 0.2 eV below the vacuum level, one may also observe a narrow feature (full width at half maxi-

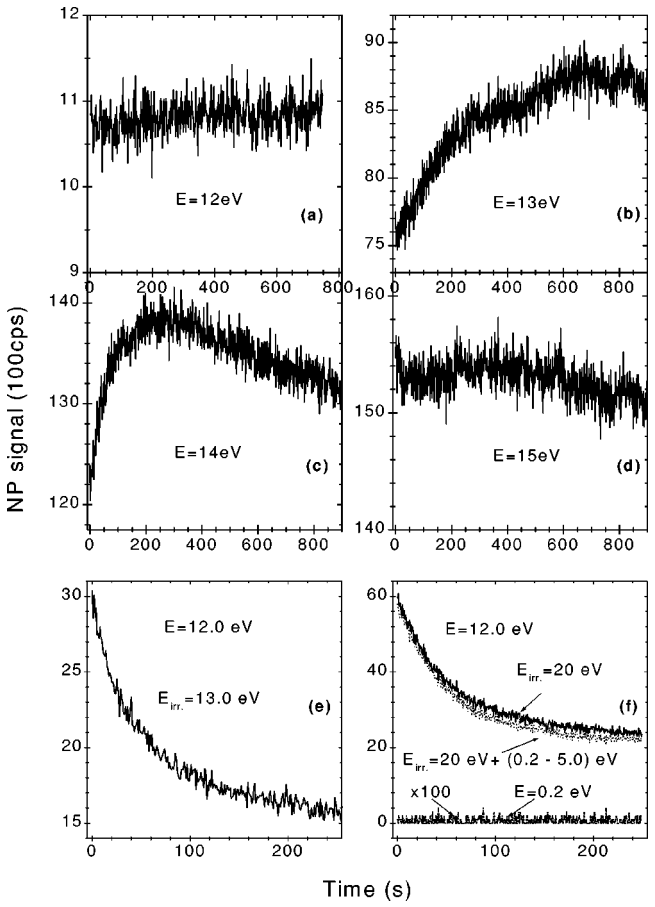

FIG. 2. Dependence of the NP signal on time of irradiation for a freshly deposited 100-monolayer (ML)-thick Ar film deposited on Pt (100 Ar/Pt) (a)–(d) and the signal initiated by 12-eV electrons from the same film preirradiated by 14-eV (e) and 20-eV (f) electrons for a period of 4 min. The lowest line in (f) is the NP signal generated by 0.2-eV electron bombardment of a pre-irradiated film (20 eV for 4 min).

mum) (<0.4 eV) at 11.5 eV associated with Ar* desorption via formation of the ^2P Ar^- electron-exciton complex.[27,29] Below 11.4 eV, negligible differences are observed between the NP yield functions from a new (i.e., nonirradiated) Ar film and a that from a bare Pt(111) surface, where the weak signal is attributable to background photons.

Figure 2 illustrates changes observed in the NP signal from a 100-ML as-deposited Ar film (i.e., no pre-irradiation) during irradiation with electrons of various incident energies [(a)–(d)] and during bombardment at 12 eV of a 100-Ar/Pt film pre-irradiated at 13 eV (e) and at 20 eV (f) for a period of 4 min. The combined signal of desorbed metastables and UV photons produced by incident electrons of $E=12$ and 15 eV [Figs. 2(a) and (d), respectively] differ in intensity, but are quite stable over the period of irradiation ($\sim$900 s). For bombardment at 13 eV incident electron energy [Fig. 2(b)], the NP signal increases over the first 400 s of irradiation (by $\approx$15% of its initial value) and then saturates. The 14-eV desorption signal [Fig. 2(c)] reaches a maximum after $\sim$300 s of bombardment and then decreases. The behavior of the NP signal produced by electrons of 15–19 eV is similar to that seen with 12- and 15-eV electrons (i.e., they are quite stable with time of bombardment) albeit of different intensity.

A drastically different behavior under electron bombardment at $E=12$ eV is observed for Ar films pre-irradiated at an electron energy $\geqslant$13 eV [Figs. 2(e) and (f)]. For example, for a 100-Ar/Pt system pre-irradiated by 13-eV electrons for 4 min [Fig. 2(e)], the NP signal is initially significantly higher than obtained without pre-irradiation, but subsequently decreases by 30% over the first 100 s of electrons. A similar effect is seen when an identical film is pre-irradiated with 20-eV electrons [Fig. 2(f)], although the initial NP signal is much greater. Note that in Figs. 2(e) and (f) the NP signal at long times approaches that seen for the nonirradiated Ar film [Fig. 2(a)]. Similar results (viz. a rapid decrease in NP yield from an elevated level) were obtained for other 100-Ar/Pt films pre-irradiated at 20 eV when bombarded with electrons of energies of between 10 and 14 eV, although both the NP intensity and its rate of decrease varied. No desorption signal from the pre-irradiated Ar film is observed when films are exposed to very low-energy (0.2–5 eV) electrons [the lowest line in Fig. 2(f)]. Irradiation with these very low-energy electrons of a pre-irradiated 100-Ar/Pt film prior to bombardment at 12 eV for 4 min does not stimulate this enhanced luminescence nor greatly effect the signal produced if subsequently irradiated with 12-eV electrons [dotted curve in Fig. 2(f)].

Time-of-flight (TOF) spectra recorded for a 100-Ar/Pt nonirradiated and pre-irradiated films at different incident energies are presented in Fig. 3. For nonirradiated films [Figs. 3(a), (c), and (e)] we observe a desorption signal only for incident electron energies above 11.5 eV [Fig. 3(c)]. As in earlier studies, the TOF spectrum is seen to consist of three structures: a photon peak at $t=0$ μs and two slower components at $\sim$50 μs (visible only for $E\geqslant 14$ eV) and $\sim$160 μs, that have been associated with the desorption of metastable Ar* via, respectively, the dissociation of excimer-like trapped excitons and the cavity expulsion of atomlike trapped excitons.[17,29,30] No significant signal is observed for incident electron energies $<$11.5 eV [Fig. 3(a)]. Figures 3(b), (d), and (f) depict the TOF spectra (at the same excitation energies shown for nonirradiated films) obtained for a 100-Ar/Pt film pre-irradiated by 20-eV electrons during 4 min. In contrast to the nonirradiated films, we observe a NP desorption signal at 9.5 eV [Fig. 3(b)]. Increasing the excitation energy also increases the desorption signal and we observe the appearance of the fast metastable component at $\sim$50 μs at excitation energies $\geqslant$11.5 eV [Figs. 3(d) and (f)]. Electron bombardment of the irradiated film over 30 s with $E=12$ eV diminishes considerably the fast component at $\sim$50 μs. It should be noted that the metastable/photon ratio for pre-irradiated films is somewhat higher than that for the as-deposited Ar films [Figs. 3(e) and (f)]. The variability of the NP signal produced by 12-eV electron bombardment of irradiated Ar films of increasing thickness (20–80 ML's) condensed onto Pt(111) or upon a 3-ML crystalline n-hexane film is illustrated in Fig. 4. For a 20-Ar/Pt film, the desorption signal is stable with exposure to the 12-eV electron [Fig. 4(a)]. For thicker Ar films on Pt(111), we observe the previ-

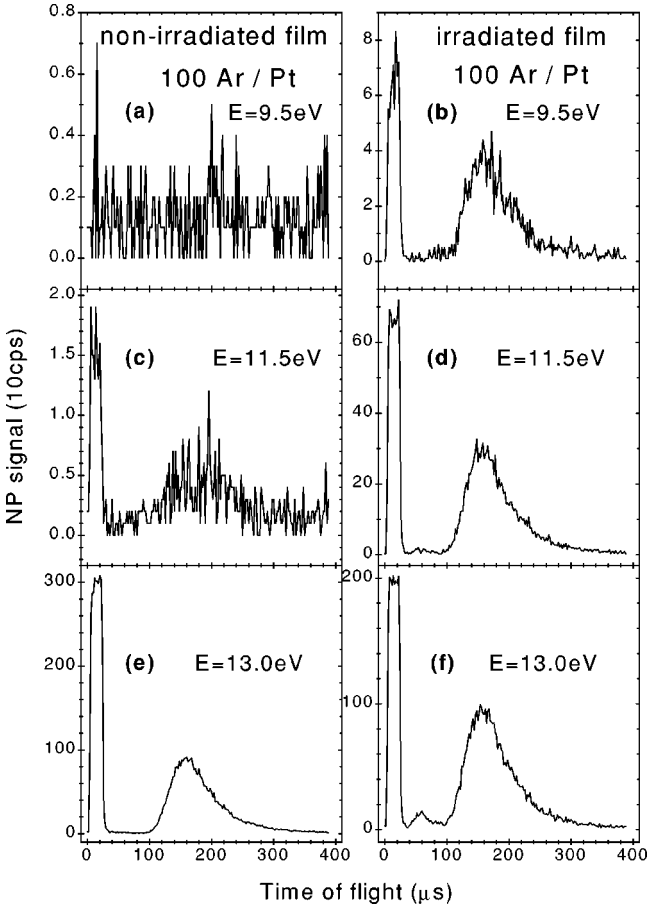

FIG. 3. Time-of-flight spectra of desorbed neutral particles obtained at the indicated electron impact energies from nonirradiated [(a), (c), (e)] and from pre-irradiated (20-eV electrons; 4 min) [(b), (d), (f)] 100-ML Ar films condensed onto Pt(111).

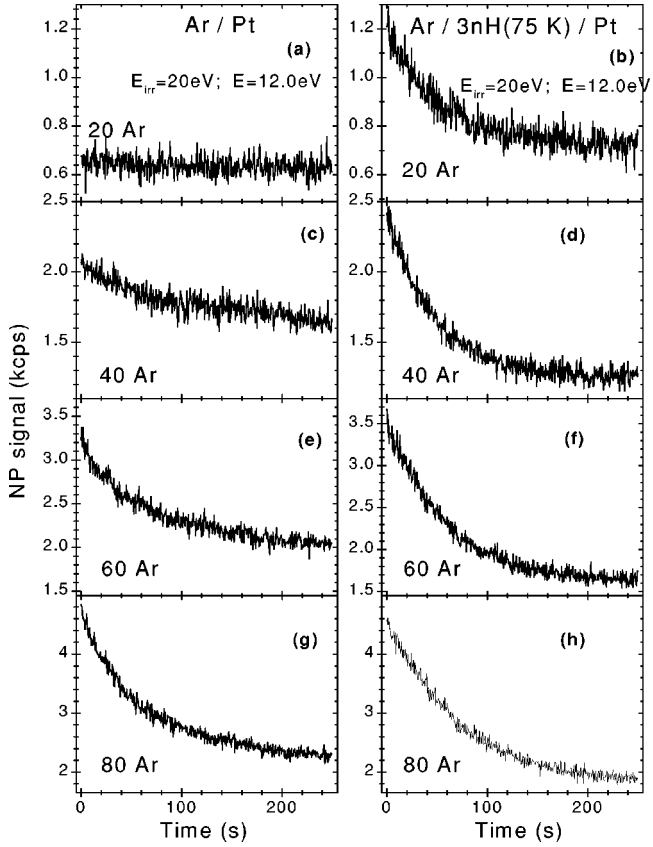

FIG. 4. Variation of the NP signal induced by 12-eV electrons from pre-irradiated (20-eV electrons; 4 min) Ar films of the indicated thicknesses deposited onto Pt(111) [(a), (c), (e), (g)] and onto a 3-ML *n*-hexane film condensed at 75 K [(b), (d), (f), (h)].

ously described decrease in NP yields with time of electron bombardment, that becomes more evident with increasing film thickness [Figs. 4(c), (e), (g)]. For Ar films condensed onto a 3-ML crystalline n-hexane, a decrease in NP signal is observed even for a 20-ML Ar film [Fig. 4(b)] and which as with the Ar/Pt system, becomes more pronounced with increased Ar film thickness [Figs. 4(d), (f), and (h)]. For the thickest Ar films (80 ML's) the variation in NP signal at $E = 12$ eV with time of exposure is almost independent of the underlying substrate [Figs. 4(g) and (h)].

These data, especially the lowering in energy of the threshold for NP production from pre-irradiated Ar films [i.e., cf. Figs. 3(a) and (b)] indicate that these luminescence and desorption phenomena are likely associated with the accumulation of positive charge within the Ar film for $E_{\mathrm{irr}} > 13$ eV. If an Ar film were to become positively charged, then the energy of incident electrons arriving at the film surface would increase relative to the case of an uncharged film by an amount eV_T, where e is the electronic charge and V_T is the potential associated with the accumulated positive charge. As a consequence, the threshold of the NP excitation function (~11.4 eV for nonirradiated Ar film as shown in the inset in Fig. 1) would appear to shift to lower energy in subsequent NP yield measurements. Figure 5 shows the near-threshold region of the NP yield function and its sensitivity to electron bombardment. The lowest curve of the figure was obtained for an uncharged 60-ML-thick film of Ar and shows an NP threshold of 11.4 eV. After 4 min bombardment at 20 eV, a new threshold [marked "60 Ar (irr.)" in the figure], approximately 1 eV lower in energy at 10.4 eV. The threshold is unaffected by the deposition of a further 60 ML's of Ar ("+60 nonirr." in the figure). However, when this 120-ML Ar film is irradiated once more for 4 min, the threshold shifts to ~9 eV. The same effect is observed when irradiating a further additional 60 ML's of Ar, where the threshold of excitation function for 180-Ar/Pt film shifts to ~7.9 eV. By analogy with our earlier experiments linking the displacement of threshold in low-energy electron transmission spectra to the accumulation of negative charge,[31,32] we propose that the displacements observed here correspond to the V_T generated by trapped charge and which seen near the film surface by incident electrons.

We have measured the NP yield functions in the range $6 < E < 13$ eV for 100-ML Ar films pre-irradiated at 20 eV, for increasing periods of time, to observe the displacement of the NP threshold and hence V_T, as a function of electron-beam exposure. The results are reported in Fig. 6 and show the dependence of this shift (measured in eV) on the bombardment time for 100-ML Ar films deposited onto Pt(111) (solid line) and onto a 3-ML crystalline *n*-hexane film con-

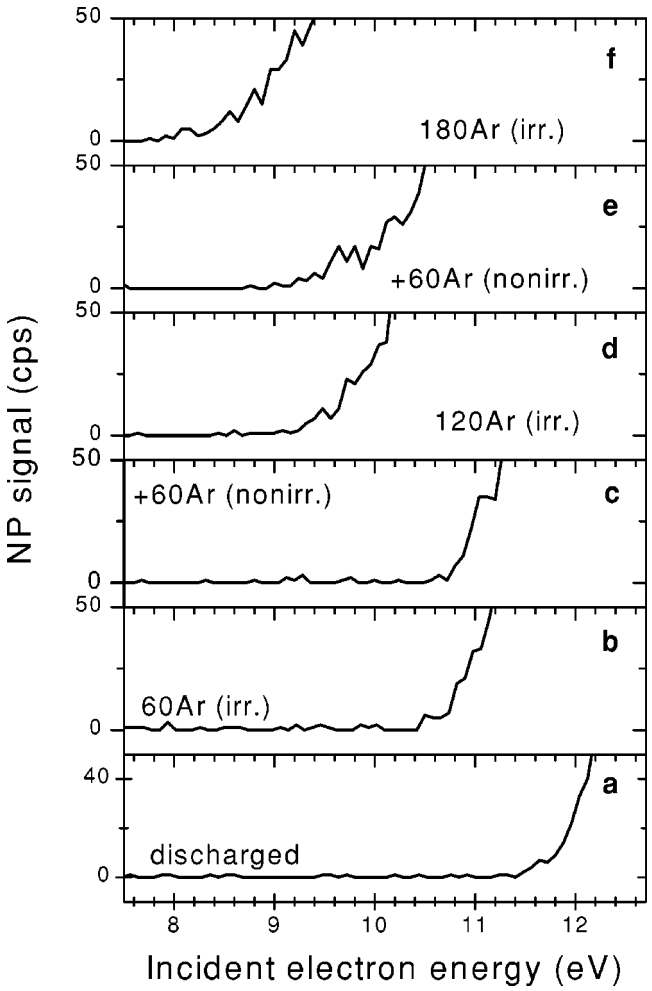

FIG. 5. The threshold region of the NP yield function for Ar films of the indicated thickness, after electron irradiation (20 eV; 4 min) [(b), (d), (f)] and after deposition of an additional nonirradiated 60 ML's of Ar [(c), (e)]. (a) The threshold of the excitation function for an uncharged film.

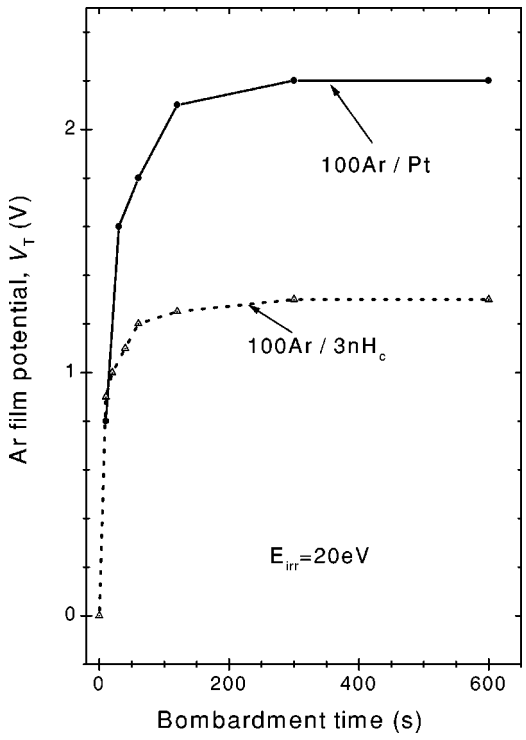

FIG. 6. Dependence of film potential V_T on bombardment time with 20-eV electrons for 100 Ar/Pt (solid line) and 100 ML's of Ar deposited on 3 ML's of crystalline *n*-hexane (100 Ar/3nH_c, dotted line).

densed at 75 K on Pt(111) (dotted line). The figure indicates that at 20 eV, thick Ar films charge rapidly reaching saturation after 3–4 min of irradiation. Also note that the asymptotic value of V_T is substantially larger for Ar films condensed onto Pt(111) than for those deposited on nH_c (2.2 and 1.3 V, relatively). It was found that electron irradiation at $E=20$ eV for even a limited period results in a significant positive charging of the 100-Ar film (~80% of its asymptotic value for 100-Ar/Pt and ~90% for 100-Ar/3nH_c after 1 min irradiation).

A related difference between Ar films grown on Pt and nH_c substrates is also evident in Fig. 7 which plots the asymptotic values of V_T reached after 4 min exposure to 20-eV electrons against Ar film thickness. It is readily apparent that the V_T displacement is linearly dependent on the thickness of the Ar film, but that the constants of proportionality for films deposited on Pt and nH_c substrates are different. The constant of proportionality is, however, independent of the thickness of the underlying nH_c film and no significant difference in V_T is observed between Ar films of identical thickness deposited onto a 3- and 10-ML nH_c.

The potential generated by electron bombardment of a 100-ML Ar film is strongly dependent on the energy of incident electrons as demonstrated in Fig. 8. Here, the solid line represents the asymptotic value of V_T as a function of *initial* incident electron energy; i.e., it ignores the increase in electron energy as positive charges accumulate in the film. The dotted line shows the asymptotic value of V_T against *final* incident electron energy (i.e., after charging). According to these data, the maximum of positive charging of the 100-Ar/Pt film is achieved with electron bombardment at energies of ~25–26 eV.

As described earlier, further irradiation of a pre-irradiated Ar film with electrons of $E<14$ eV produces an intense NP signal that diminishes with electron dose [Figs. 2(e) and (f)]. The strength of this transient-stimulated emission/desorption is strongly dependent on the energy of incident electrons. Figure 9 plots the initial rate of decay of the stimulated luminescence/desorption (solid line) as a function of electron energy for a 100-Ar/Pt film pre-irradiated by 20-eV electrons. It was found that the maximum decay rate was observed with ~12-eV incident energy electrons and that similar but smaller effects are also observed at 13 and ~13.6 eV. The curve illustrated in Fig. 9 bears a strong resemblance to the photon adsorption spectrum,[33] reproduced at the top of the figure. The sharp structures seen in this later indicate ''resonant'' excitation of surface and bulk exciton states.

It was also found that films positively charged by pre-irradiation at 20 eV could, by further electron irradiation at 12 eV for 2–3 min, return the NP threshold to its initial

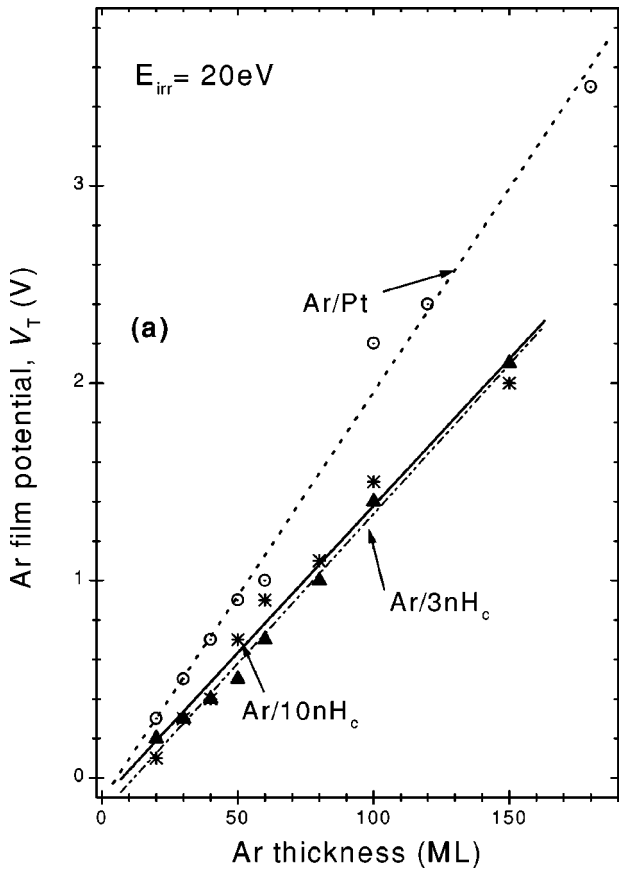

FIG. 7. Dependence of potential V_T of an Ar film as a function of its thickness. Circles: Ar film deposited onto Pt(111); stars and triangles: Ar film deposited on a 3-ML and a 10-ML *n*-hexane layer condensed at 75 K.

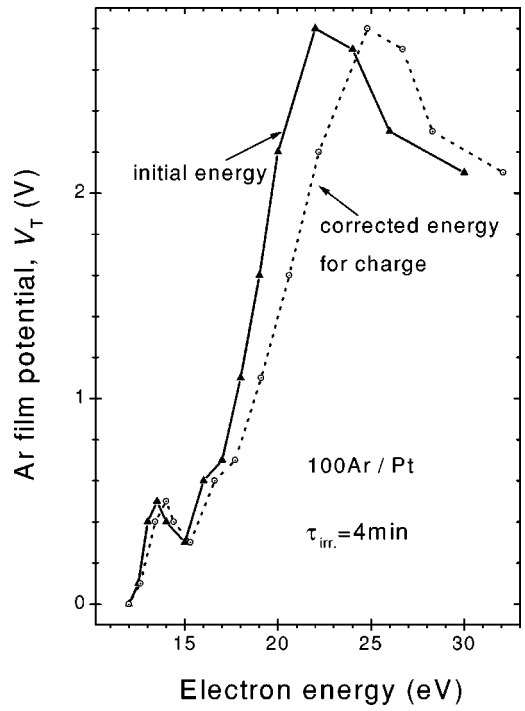

FIG. 8. Variation of V_T of a 100-Ar/Pt film induced by 4 min of electron bombardment at energies $11<E<32$ eV; solid line: as a function of the initial energy of incident electrons; dotted line: as a function of the final electron energy (i.e., taking into account film charging).

energy, i.e., to 11.4 eV. The data of Fig. 9 also illustrate the sensitivity of this ''discharging'' process on incident electron energy. The dotted line presents the change of V_T (ΔV_T) seen for a pre-irradiated (20 eV, 4 min) 100-Ar/Pt film after a discharging bombardment for 4 min with electrons of different energies. The procedure was the following: the Ar film was irradiated with 20-eV electrons for 4 min, after which time the energy of the NP threshold was determined. Next, the film was irradiated with electrons of one specific energy (between 0 and 13.6 eV) for 4 min and again the NP threshold energy was located. In each case, the time required to measure the NP yield function (and hence the NP threshold) was ~3 s, a time too short to greatly effect the quantity of positive charge accumulated in the film. We estimate that the error introduced by such measurements was less than 0.1 eV. It is clearly seen that no significant discharge of the pre-irradiated Ar film is produced by electron exposure at $E \leqslant 5$ eV (the dotted line). At higher electron energies, the efficiency of the discharging process increases and reaches its maximum at 12 eV, the same energy at which the maximum stimulated emission is observed (solid line). When comparing these data for stimulated NP production and for ΔV_T, it is should be noted that those for NP production represent ''differential'' measurements, reporting changes occurring within a few seconds of electron irradiation. In contrast, measurements of ΔV_T are integrated over 4 min, which may increase sensitivity to weak (slow) discharge processes at the expense of sensitivity to more efficient rapidly occurring phenomena.

DISCUSSION

The experimental results presented above, in particular the reversible shift to lower energy of the threshold of NP production with irradiation by electrons with $E_{\mathrm{irr}} \geqslant 13$ eV, demonstrate both the creation and stabilization of positive charge in the film and its neutralization by electron bombardment.

Charge stabilization

It is known that following irradiation with electrons (or photons) with energies greater than the gap E_g, electrons and holes are generated, e.g.,

$$\mathrm{Ar} + e^- \rightarrow \mathrm{Ar}^+ + 2e^-. \quad (1)$$

The holes rapidly trap as molecular cations with a consequent release of energy to the lattice,[9,34] i.e.,

$$\mathrm{Ar} + \mathrm{Ar}^+ \rightarrow \mathrm{Ar}_2{}^+ + \Delta E. \quad (2)$$

Positive charges may also be trapped by ionization of impurities, either directly by electron impact, or indirectly by energy transfer from Ar excitons. However, the high purity of Ar used in our experiments (99.9995%) and ultrahigh

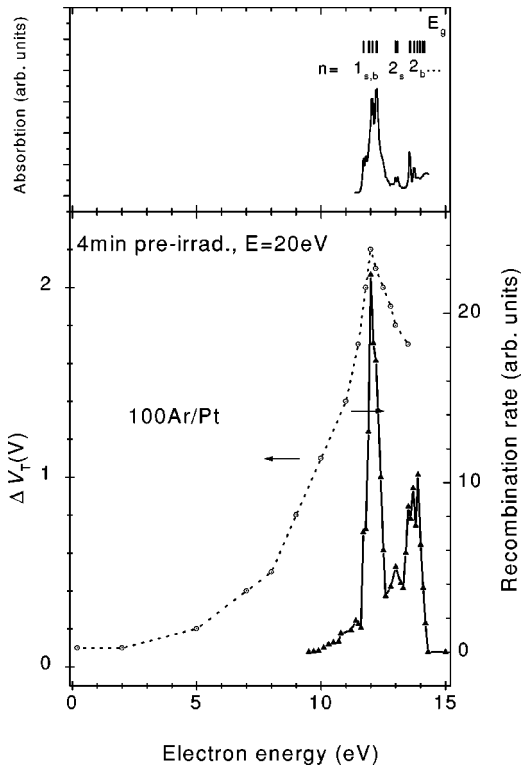

FIG. 9. Lower panel: Electron energy dependence of the rate of decay of the transient NP signal (solid line) and the change ΔV_T of the potential of a 100-Ar/Pt pre-irradiated film after 4 min of electron bombardment (dotted line). Upper panel: Excitonic structure seen in the photon absorption spectrum of thick Ar films, taken from Ref. 33; energetic positions of excitonic bands and gap energy are indicated at the top.

vacuum (4×10^{-11} torr) substantially diminishes the possibility that these effects are dominant. Moreover, in Figs. 3(e) and (f), one observes that the photon/metastable ratio is higher for non-pre-irradiated films than for irradiated ones (3 and 2, relatively). If impurities did substantially influence the trapping process, one would expect to observe an increase of the photon component of NP signal from the pre-irradiated films that would be associated with the neutralization of ionized impurities. However, such impurities could not be expected to contribute to the desorption signal of metastables, since their distinct electronic structure should not initiate an Ar exciton, the trapping of which is necessary for desorption.

Nevertheless, our experiments demonstrate that positive charge accumulation (and thus ionization) can be initiated in Ar films condensed on Pt by electron bombardment at energies as low as 13–14 eV, i.e., substantially below $E_g = 14.16$ eV.[1,26] In fact, ionization with 14-eV electron bombardment is not so very surprising, since it has already been demonstrated[35] that the ionization limit for the surface excitons for Ar/Pt film is $E_T^S = 13.66$ eV (compared with 14.16 eV in the bulk and 15.75 eV in vacuum). Hence 14-eV electrons may generate free holes and electrons in *pure* Ar films. The ionization of the Ar film as the result of bombardment at 13-eV electrons may be explained by ionization of excitons trapped by defects in Ar film or by impurities.[7,13] Indeed, the existence of a noncompensated localized hole will accelerate a passing electron resulting in an increase of its energy and hence promote the ionization of another Ar atom.

The accumulation of positive charges in the 100-Ar/Pt film explains the interesting behavior of the NP yield observed with increased dose of the 13-eV electrons, as shown in Fig. 2(b). Note that in Fig. 1, the NP desorption signal rises with incident electron energy over the range 12–14 eV. Since (as argued above) 13-eV electrons may create holes that stabilize within the film, bombardment at 13 eV charges the film positively, so that later arriving electrons are accelerated to higher energies capable of generating a larger desorption signal. The complex behavior of the 14-eV desorption signal [Fig. 2(c)] may be explained by the existence of several competing processes, such as (i) direct exciton creation; (ii) interaction of incident electrons with trapped holes; (iii) recombination of slow electrons with holes; and (contrary to the 13-eV signal) (iv) generation of free charge carriers that becomes possible due to the ~0.4-V increase of the film's potential (Fig. 8). Thus the energy of impinging electrons rapidly exceeds $E_g = 14.16$ eV. The complexity of these competing processes occurring in the threshold range of the E_g is also confirmed by the anomalous small decrease of the film potential produced by the electron bombardment within the 14–15-eV range (Fig. 8).

Charge neutralization and stimulated NP production

Positive charge can contribute to the luminescence and/or NP desorption yields in two distinct ways:
(i) By recombination with electrons, viz.

$$\mathrm{Ar_2}^+ + e^- \rightarrow \mathrm{Ar}^* + \mathrm{Ar} + (\Delta E). \tag{3}$$

The resulting excited Ar* (or exciton) is subsequently subject to the same trapping and decay processes experienced by excitons created directly from electron (or photon) bombardment at energies below E_g. That is, it may with low probability decay immediately, or more probably, trap as an *m*-STE or *a*-STE center prior to photon emission, metastable emission or excimer ejection.
(ii) By exciton trapping: Stable molecular ions may capture excitons to form an excited state that decays by light emission in the *H* band in the near-UV region.[36,37] The process can be summarized as follows:

$$\mathrm{Ar_2}^+ + (\mathrm{exciton}) \rightarrow (\mathrm{Ar_2}^+)^* \rightarrow \mathrm{Ar}^+ + \mathrm{Ar} + h\nu(H \ \ \mathrm{band}). \tag{4}$$

The *H* band is centered at ~6.2 eV with a half width of ~0.7 eV and such photons lie close to the energetic threshold for detection with the microchannel plate assembly. It is unlikely, then, that this luminescence signal is detected with great efficiency in the present experiments.

Exciton trapping is expected to be most efficient at incident energies close to E_g. Ogurtsov *et al.*,[37] after Ratner,[38] reported that the cross section for exciton trapping σ_i is given by

$$\sigma_i \cong \frac{1.5\rho^2}{\sqrt{T}}, \tag{5}$$

where T is the temperature and ρ is the radius of the exciton, both in atomic units, and ρ is determined by the quantum number n of the excited shell. For $n=1$ excitons, ρ is close to 5 a.u., while for $n=3$, $\rho=40$ a.u. Thus for $n=3$ excitons at 20 K, σ_i is $\sim 8\times 10^{-12}$ cm^2, approximately 2 orders of magnitude greater than for $n=1$ excitons (1.2×10^{-13} cm^2). These are both large cross-section values, nevertheless, it should be noted that the *M*-band luminescence signal (from electron-Ar_2^+ recombination) is several times stronger than the *H*-band signal in the photoinduced luminescence spectra of pre-irradiated Ar films, from $h\nu = 11-20$ eV.[37]

It is especially important to note that contrary to the case of electron-hole recombination, *exciton capture cannot reduce the quantity of positive charge trapped in an Ar film*. Moreover, it has been shown by Baba *et al.*[39] that positive ion desorption is not observed from Ar films for electron impact energies below 24.2 eV. Hence, for nearly the entire range of incident electron energies employed in this study, *electron-hole recombination represents the sole process capable of discharging the Ar films*.

The transient stimulated production of NP's from pre-irradiated Ar films under low-energy electron bombardment is seen from Fig. 9 to be most efficient at $E=12$ eV and otherwise highly correlated with the energetic thresholds of Ar* excitons as determined by photon absorption measurements. This energy is coincidentally the same one at which the discharge process is most efficient (dotted curve in Fig. 9). Consequently we propose that both phenomena viz. the decrease in V_T and the stimulated production of NP derive from, or are dominated by, a single process, namely the recombination of Ar_2^+ centers with low-energy electrons.

We have already argued that in this energy regime, only electron-Ar_2^+ recombination is capable of reducing the accumulated positive charge, but why should recombination be more efficient at 12-eV incident electron energy than at lower energies (down to 0.2 eV)? The answer is that only electrons of near-thermal energies in the film can recombine efficiently with the Ar_2^+ centers. The absence of energy-loss processes in the film below the threshold of the $n=1$ surface and bulk excitons at 11.71 and 12.04, respectively,[26] and the (related) long mean free path of low-energy electrons in Ar (Ref. 40) militate against thermalization even for incident electrons with nominal energies as low as 0.2 eV. Additionally, the presence of a positive potential V_T accelerates incident electrons limiting our ability to irradiate the film with near-thermal energy electrons. However, for incident electrons with just sufficient energy to excite an exciton, electron scattering produces not only the Ar*, but also a very-low-energy electron, capable of participating in recombination process (3). It is for this reason that the transient-stimulated NP production is also most intense at energies corresponding to an exciton threshold. Indeed, it is the observation of sharp structures in NP production data of Fig. 9 that demonstrates that this signal derives principally from recombination rather than the capture of excitons. This is because in electron impact experiments and contrary to photon measurements, the cross sections for exciton production increase with electron energy, above their thresholds.[20,35] Similarly, if exciton capture were the dominant process leading to *H*-band luminescence and hence NP production, one would not observe ''threshold'' peaks but rather a much more smoothly rising signal.

Finally, we note that the data presented in Fig. 8 report measurements relating stabilization of Ar_2^+ with incident electron energy. The curve, however, is not proportional to the cross section for hole production, since stabilization is modulated by other processes occurring within the film including prompt recombination, electron transmission to substrate, electron emission, and exciton capture, all of which may vary with the initial energy of the incident electron beam and the residual energies of scattered electrons.

Charge stability and localization

The results presented in Figs. 5–7 clearly demonstrate that electron bombardment with $E \geqslant 13$ eV results in a positive charging of Ar films and further permit study of their stability, localization, and ability to diffuse within the film. This is significant since even the existence of the stable self-trapped holes in RGS's has not been experimentally confirmed with certainty.[16] Electron bombardment with $E \geqslant 13$ eV of an Ar film results in the shift of the excitation function threshold to lower energy (Fig. 5). As the deposition of additional Ar layers does not change the position of this threshold, one must conclude that *self-trapped holes are immobile* (at 20 K) and no significant displacement towards the new interface film/vacuum is observed. The stability of self-trapped holes has been previously determined at lower temperatures (<10 K) by thermoluminescence.[41]

In principle, positive charge may stabilize principally within the bulk of the film, or close to the film's surface or some combination of these extremes. Despite the relatively slow and gentle conditions of Ar film deposition in our experiments (5 ML's/min and $T=20$ K, i.e., close to the sublimation temperature) that promote the formation of relatively defect-free Ar films, it is still possible that charge might stabilize within the bulk of irradiated Ar film. It has been shown[41,42] that the excitation of the electron subsystem of atomic RGS's causes a considerable rearrangement of the crystal lattice and leads to the formation of stable point defects in the structure. Such defects may serve as traps of the charge carriers.

We may consider the positively charged Ar film as a charged capacitor, since the thickness-to-radius ratio is very small.[31] In the case of a uniform charge distribution within the Ar layer, the potential inside the film as a function of distance from the substrate z is given by

$$V(z)=\rho z(d-z/2)/(\varepsilon\varepsilon_o), \tag{6}$$

where ρ is the charge density trapped in the volume, d the film thickness, ε the static dielectric constant (for Ar, $\varepsilon=1.56$), and ε_o the permitivity of vacuum, 8.854×10^{-14} C V^{-1} cm^{-1}. Hence the surface potential V_T in volts increases quadratically with the thickness of the Ar layer:[7]

$$V_T=0.9\times 10^{-6}\rho d^2/\varepsilon. \tag{7}$$

In the case of a uniform distribution of charges at the surface of the Ar film, the surface potential for a film thickness d in cm is given by[7]

$$V_T = 1.81 \times 10^{-6} \sigma d/\varepsilon,$$

where σ is charge density in q/cm^2 (q is the elementary charge). Here, the surface potential is expected to increase linearly with the film thickness. The linear dependence between V_T and Ar film thickness (Fig. 7) indicates that the main part of the positive charge is localized at the surface of the Ar film or within a relatively thin surface layer. This conclusion corroborates well the results of Reimann *et al.*[15] that the hole trapping probability at the vacuum interface is larger than the bulk trapping. In the case of the surface potential $V_T = 2.2$ V for a 100-Ar/Pt film irradiated by 20-eV electrons (Fig. 6), and according to the published data for the nearest-neighbor distance for Ar fcc lattice,[26] the surface charge is $\sigma = 5.05 \times 10^{11} q/\mathrm{cm}^2$ which corresponds to a concentration of $\sim 6 \times 10^{-4}$ holes per surface atom. For Ar films condensed onto crystalline *n*-hexane, we also observe a linear dependence of V_T on the film thickness (Fig. 7), i.e., for the Ar/nH_c system the positive charge is also localized at the surface of the Ar film.

Differences between Pt and nH_c substrates

The lower values of V_T developed in Ar films deposited on nH_c, relative those seen for films deposited directly on Pt, likely reflect an increased rate of electron-Ar_2^+ recombination in the former case that limits positive charge accumulation. A physical basis for this phenomena may lie in the higher "V_0" level of *n*-hexane [0.8 eV (Ref. 43)] relative to that of Ar (0.3 eV) that could increase recombination by impeding the passage of very low-energy electrons through to the Pt substrate. Support for this explanation is provided by the independence of V_T with the thickness of the underlying *n*-hexane spacer (Fig. 7).

At first sight, the enhancement in the transient NP signal from thin Ar films on nH_c relative to that observed from Ar on Pt (Fig. 4) seems contradictory to the results of Figs. 6 and 7, that show lower positive charge accumulation in the former situation. However, this too may be, at least in part, explained by an increase in the electron-Ar_2^+ recombination rate, owing to an enhanced density of low-energy electrons, generated by exciton creation and impeded from transfer to the metal, by the *n*-hexane barrier. Thus the transient signal appears stronger at short times due to more rapid recombination.

CONCLUSION

Positive charge creation and annihilation induced by low-energy electron impact in thin Ar films (20–180 monolayers) has been investigated within the 5–30-eV range by measuring the desorption of metastable particles, the emission of UV photons and the threshold energies for these processes. These techniques have allowed the investigation of the dependence on incident electron energy of positive charge stabilization. This latter is not directly proportional to either the cross section for hole creation or that for hole Ar_2^+ formation, since it is also dependent on electron-Ar^+ and electron-hole recombination processes, the efficiencies of which are somewhat dependent on film thickness and the nature of the underlying substrate. Nevertheless, this measurement alone should be of value in modeling energy deposition processes occurring in thin Ar films.

We have also found that, in agreement with earlier work,[7,15] positive charge accumulation occurs principally at the film/vacuum interface. Moreover, stabilized charges are long-lived and do not migrate from their original position once Ar overlayers are added to the film.

Positively charged films can be discharged by electron bombardment, most efficiently at energies close to 12 eV. Discharging proceeds via electron-Ar_2^+ recombination and is accompanied by a transient enhancement in metastable desorption and UV photon emission initiated by exciton creation within the film. Recombination is especially strong when the incident electron energy corresponds to the threshold energy of Ar exciton states since under this condition the exciton formation simultaneously produces a thermal-energy electron that is efficiently captured by Ar_2^+ centers.

ACKNOWLEDGMENTS

Research was supported by Canadian Institutes of Health Research. We wish to thank M. Michaud for his interest and valuable comments regarding this work.

*Electronic address: Evgueni.Vichnevetski@USherbrooke.ca
†Canada Research Chair In Radiation Sciences.

[1] *Self-Trapped Excitons*, edited by K. S. Song and R. T. Williams, 2nd ed., Springer Series in Solid-State Sciences No. 105 (Springer-Verlag, Berlin, 1996).
[2] A. Hoshino, T. Hirayama, and I. Arakawa, Appl. Surf. Sci. **70–71**, 308 (1993).
[3] A. N. Ogurtsov, E. V. Savchenko, J. Becker, M. Runne, and G. Zimmerer, J. Lumin. **76–77**, 478 (1998).
[4] E. V. Savchenko, O. N. Grigorashchenko, O. M. Sokolov, J. Agreiter, N. Caspary, A. Lammers, and V. E. Bondybey, J. Electron Spectrosc. Relat. Phenom. **101–103**, 377 (1999).
[5] J. M. Warman, K. J. Smit, S. A. Jonker, J. W. Verhoeven, H. Oevering, J. Kroon, M. N. Paddon-Row, and A. M. Oliver, Chem. Phys. **170**, 359 (1993).
[6] *Electrets, Charge Storage and Transport in Dielectrics*, edited by M. M. Perlman (Electrochemical Society, Princeton, NJ, 1973).
[7] R. A. Baragiola, M. Shi, R. A. Vidal, and C. A. Dukes, Phys. Rev. B **58**, 13 212 (1998).
[8] E. V. Savchenko, O. N. Grigorashchenko, A. N. Ogurtsov, V. V. Rudenkov, G. B. Gumenchuk, M. Lorenz, M. Frankowski, A. M. Smith-Gicklhorn, and V. E. Bondybey, Surf. Sci. **507–510**, 754 (2002).
[9] O. N. Grigorashchenko, A. N. Ogurtsov, E. V. Savchenko, J. Becker, M. Runne, and G. Zimmerer, Surf. Sci. **390**, 277 (1997).
[10] E. V. Savchenko, O. N. Grigorashchenko, A. N. Ogurtsov, V. V. Rudenkov, G. B. Gumenchuk, M. Lorenz, A. Lammers, and V. E. Bondybey, J. Low Temp. Phys. **122**, 379 (2001).

[11] L. Sanche and M. Deschênes, Phys. Rev. Lett. **61**, 2096 (1988).
[12] J. Becker, O. N. Grigorashchenko, A. N. Ogurtsov, M. Runne, E. V. Savchenko, and G. Zimmerer, J. Phys. D **31**, 749 (1998).
[13] D. E. Grosjean, R. A. Baragiola, and W. L. Brown, Phys. Rev. Lett. **74**, 1474 (1995).
[14] A. Schrimpf, C. Boekstiegel, H.-J. Stockmann, T. Bornemann, K. Ibbeken, J. Kraft, and B. Herkert, J. Phys.: Condens. Matter **8**, 3677 (1996).
[15] C. T. Reimann, W. L. Brown, and R. E. Johnson, Phys. Rev. B **37**, 1455 (1988).
[16] M. Kink, R. Kink, V. Kisand, J. Maximov, and M. Selg, Nucl. Instrum. Methods Phys. Res. B **122**, 668 (1997).
[17] G. Leclerc, A. D. Bass, A. Mann, and L. Sanche, Phys. Rev. B **46**, 4865 (1992).
[18] E. Vichnevetski, P. Cloutier, and L. Sanche, J. Chem. Phys. **110**, 8112 (1999).
[19] G. Perluzzo, G. Bader, L. G. Caron, and L. Sanche, Phys. Rev. Lett. **55**, 545 (1985).
[20] G. Leclerc, A. D. Bass, M. Michaud, and L. Sanche, J. Electron Spectrosc. Relat. Phenom. **52**, 725 (1990).
[21] E. Vichnevetski and L. Sanche, Langmuir **15**, 6851 (1999).
[22] A. Mann, P. Cloutier, D. Liu, and L. Sanche, Phys. Rev. B **51**, 7200 (1995).
[23] G. Perluzzo, L. Sanche, C. Gaubert, and R. Baudoing, Phys. Rev. B **30**, 4292 (1984).
[24] M. Michaud, P. Cloutier, and L. Sanche, Phys. Rev. B **44**, 10 485 (1991).
[25] L. Sanche, J. Chem. Phys. **71**, 4860 (1979).
[26] N. Schwentner, E.-E. Koch, and J. Jortner, *Electronic Excitations in Condensed Rare Gases* (Springer-Verlag, Berlin, 1985).
[27] A. D. Bass, E. Vichnevetski, P. Cloutier, and L. Sanche, Phys. Rev. B **57**, 14 914 (1998); **60**, 5078(E) (1999).
[28] S. J. Buckman and C. W. Clark, Rev. Mod. Phys. **66**, 539 (1994).
[29] A. D. Bass, E. Vichnevetski, and L. Sanche, Phys. Rev. B **60**, 14 405 (1999).
[30] G. Zimmerer, Nucl. Instrum. Methods Phys. Res. B **91**, 601 (1994).
[31] R. M. Marsolais, M. Deschênes, and L. Sanche, Rev. Sci. Instrum. **60**, 2724 (1989).
[32] K. Nagesha, J. Gamache, A. D. Bass, and L. Sanche, Rev. Sci. Instrum. **68**, 3883 (1997).
[33] V. Saile, M. Skibowski, W. Steinmann, P. Gurtler, E. E. Koch, and A. Kozevnikov, Phys. Rev. Lett. **37**, 305 (1976).
[34] G. Zimmerer, J. Low Temp. Phys. **111**, 629 (1998).
[35] M. Michaud and L. Sanche, Phys. Rev. B **50**, 4725 (1994).
[36] A. N. Ogurtsov, E. V. Savchenko, M. Kirm, B. Steeg, and G. Zimmerer, J. Electron Spectrosc. Relat. Phenom. **101–103**, 479 (1999).
[37] A. N. Ogurtsov, A. M. Ratner, E. V. Savchenko, V. Kisand, and S. Vielhauer, J. Phys.: Condens. Matter **12**, 2769 (2000).
[38] A. M. Ratner, Phys. Rep. **269**, 197 (1996).
[39] Y. Baba, G. Dujardin, P. Feulner, and D. Menzel, Phys. Rev. Lett. **66**, 3269 (1991).
[40] T. Goulet, J.-M. Jung, M. Michaud, J.-P. Jay-Gerin, and L. Sanche, Phys. Rev. B **50**, 5101 (1994).
[41] E. V. Savchenko, A. N. Ogurtsov, O. N. Grigorashchenko, and S. A. Gubin, Low Temp. Phys. **22**, 926 (1996).
[42] E. V. Savchenko, A. N. Ogurtsov, O. N. Grigorashchenko, and S. A. Gubin, Chem. Phys. **189**, 415 (1994).
[43] L. G. Caron, G. Perluzzo, G. Bader, and L. Sanche, Phys. Rev. B **33**, 3027 (1986).